American Mineralogist, Volume 62, pages 913–920, 1977

Cation distribution and high-temperature crystal chemistry of armalcolite

BARRY A. WECHSLER

Department of Earth and Space Sciences
State University of New York
Stony Brook, New York 11794

Abstract

The structures of two synthetic armalcolite crystals of composition $Fe_{0.5}Mg_{0.5}Ti_2O_5$ have been refined at temperatures between 24° and 1100°C. At room temperature after quenching from 1200°C, mean M–O distances suggest the presence of substantial cation disorder. Annealing at ~400°C for 24 hours resulted in expansion of $\langle M1\text{–O}\rangle$ and contraction of $\langle M2\text{–O}\rangle$ distances measured at room temperature. This indicates that intracrystalline diffusion took place at 400°C, yielding an essentially completely ordered cation distribution. The refined structure at 400°C shows similar trends. At 1100°C, cation disorder reappeared, and $\langle M1\text{–O}\rangle$ was more similar to $\langle M2\text{–O}\rangle$ than at room temperature or 400°C. Unit-cell parameters also reflect the degree of cation ordering. These observations are consistent with stabilization at high temperatures due to configurational entropy.

Introduction

The mineral armalcolite is of interest because of its implications for the petrogenesis and cooling history of the lunar rocks in which it is found. Its chemical and textural trends can be used to define the temperature–pressure–oxygen fugacity conditions during crystallization of the lunar basalt melts (see, for example, Haggerty, 1973; El Goresy *et al.*, 1974; Papike *et al.*, 1974; Kesson and Lindsley, 1975). Armalcolite ($Fe_{0.5}Mg_{0.5}Ti_2O_5$) is essentially a solid solution between $FeTi_2O_5$ (ferropseudobrookite) and $MgTi_2O_5$ (karrooite) which is unstable below 1010 ± 20°C (Lindsley *et al.*, 1974), but the presence of Al_2TiO_5, Cr_2TiO_5, and Ti_3O_5 in solid solution stabilizes the mineral to lower temperatures (Kesson and Lindsley, 1975).

Armalcolite has the pseudobrookite structure, and its crystallographic features have been described previously by Lind and Housley (1972), Smyth (1974), and Wechsler *et al.* (1976). Lind and Housley suggested an essentially completely-ordered cation distribution in synthetic armalcolite. However, the latter two studies indicated that cation disorder might exist in quenched synthetic samples, although lunar armalcolites were found to be highly ordered. Virgo and Huggins (1975) confirmed Fe^{2+} disorder in a quenched synthetic armalcolite by Mössbauer techniques. Navrotsky (1975) favored the presence of cation disorder at high temperatures in similar minerals, and suggested that these phases were actually stabilized by the entropy associated with cation disorder.

In order to understand the partitioning behavior and stability relations of armalcolite and related minerals, high-temperature crystal-structure data are useful. The present study was undertaken to document the effects of cation disorder and thermal expansion on the armalcolite structure.

Experimental procedures

Synthesis of samples

Two different synthetic armalcolite samples were utilized in the experiments reported here. Both samples were synthesized in evacuated silica-glass tubes from oxide mixtures following the procedures outlined by Lindsley *et al.* (1974) to yield a single phase of composition $Fe_{0.5}Mg_{0.5}Ti_2O_5$. Run times of ~5 days at 1200°C yielded crystals of approximately 0.1–0.5 mm in the maximum dimension, elongated along the c axis. Samples were quenched rapidly from 1200°C. The crystal referred to as Arm-C was taken from a run using the same mix of composition $Fpb_{50}Kar_{50}$ which was used in the experiments of Lindsley *et al.* (1974). The crystal called Arm-E was taken from a run using a different mix, but was

designed to be of the same composition as Arm-C. A room-temperature refinement of the structure of Arm-C has previously been reported by Wechsler *et al.* (1976), where this crystal was designated $Fpb_{50}Kar_{50}$.

Precession camera studies

Two crystals were studied by X-ray precession techniques to determine the thermal stability of armalcolite under the conditions imposed by the experimental plan. The first crystal was subjected to heating at 400°, 600°, and 800°C for 24 hours each and briefly at 1050°C while 0*kl* precession photos were exposed. In addition, *h*0*l* and 0*kl* photos were taken at room temperature both before and after the heating cycle. The initial room-temperature photos and the 400°C photo show a single-phase armalcolite with sharp reflections. At 600° the reflections appeared somewhat diffuse, and at 800°C further diffuseness was accompanied by the appearance of two new phases, anatase and rutile. These are in an oriented relationship with the host armalcolite. Several related orientations of rutile were found, with the predominant one having $(001)_{rut}$ parallel to $(100)_{arm}$, and $(110)_{rut}$ parallel to $(010)_{arm}$ and $(001)_{arm}$. The (100) or (010) of anatase was parallel to $(001)_{arm}$, and (101) or (011) of anatase was parallel to $(010)_{arm}$. After heating the crystal at 1050°C for about two hours followed by quenching to room temperature, the rutile reflections became more intense relative to the anatase reflections. No other phases were identified among the breakdown products. Microprobe analysis of the crystal after the heating experiment was consistent with slight oxidation of the sample, which could account for the appearance of TiO_2 without accompanying ilmenite. However, it is unlikely that oxidation was the result of a crack in the sealed, evacuated silica-glass capillary in which the crystal was heated. Rather, a possible reaction with the high-temperature cement and/or remaining oxygen in the capillary is preferred to explain the armalcolite decomposition.

A second synthetic armalcolite crystal was studied on a precession camera in a cycle consisting of room temperature, rapid heating directly to 1100°, exposure at 1100°C for 24 hours, and rapid cooling back to room temperature. The quality of the armalcolite reflections was not affected, and only a single phase was present at all times, including room temperature after heating. The lack of reaction during this experiment suggests that armalcolite stability was achieved. Rapid heating and quenching (in a period of less than ten minutes) through the lower temperature range in which the armalcolite was not a stable phase was sufficient to avoid noticeable breakdown of the crystal.

Structure refinements

Two additional synthetic armalcolite crystals were studied on an automated Picker four-circle diffractometer with Mo$K\alpha$ radiation and a graphite monochromator. The crystal labelled Arm-C was subjected to heating at 400°, 600°, 800°, and 1050°C, while Arm-E was heated only at 1100°C. Three-dimensional X-ray intensity data were collected at each temperature as well as at room temperature both before and after heating. Two sets of room-temperature data were collected on Arm-E, one prior to mounting the crystal for high-temperature study and a second following the high-temperature mounting. Since the mounting process included heating at ~400°C for 24 hours, the difference between these two data sets represents the effects due to annealing at this temperature. Because decomposition of the crystal Arm-C occurred after data collection at 400°C, the subsequent data sets for this crystal will not be considered further here.

All reflections with 2θ between 5° and 70° were measured in one quadrant of reciprocal space for Arm-C. Intensities were corrected for background, Lorentz, and polarization factors; and structure factors of equivalent reflections were averaged to reduce the data to a set of unique reflections. For Arm-E, only reflections in one octant of reciprocal space were measured, in order to minimize the period of heating required. After data collection was completed, the 2θ values of from 15 to 21 reflections were measured accurately, and the average of the positive and negative 2θ-angles measured for each was used in a least-squares refinement of the unit-cell parameters (Table 1).

The crystal Arm-C measured ~0.2 × 0.2 × 0.28 mm. An attempt to apply an absorption correction to its data was made but resulted in no significant change in positional parameters and no improvement in the *R*-factors determined during structure refinements. The results reported here are for the non-absorption corrected data. No absorption correction was applied to the data for Arm-E, which measured ~0.08 × 0.08 × 0.10 mm. The lack of an absorption correction is not expected to have significantly affected the results, although temperature factors for the refinements might be slightly affected.

During data collection of Arm-E at 1100°C, the intensity of a standard reflection (632), measured af-

Table 1. Unit-cell parameters and ⟨*M*–O⟩ distances of synthetic armalcolite

	Arm-E				Arm-C	
	24°C before annealing	24°C after annealing	1100°C	24°C after heating	24°C*	400°C
a(Å)	9.7762(3)†	9.7454(5)	9.899(1)	9.7697(7)	9.7762(4)	9.7655(4)
b(Å)	10.0341(3)	10.0625(4)	10.1835(7)	10.0410(7)	10.0214(4)	10.0762(4)
c(Å)	3.7504(2)	3.7422(1)	3.7645(3)	3.7473(1)	3.7485(1)	3.7429(1)
V(Å^3)	367.89(2)	366.97(2)	379.51(4)	367.60(3)	367.25(2)	368.30(2)
<M1-O>(Å)	2.069	2.103	2.078	2.071	2.065	2.098
<M2-O>(Å)	1.994	1.979	2.023	1.994	1.993	1.986

**Data for Arm-C at 24°C taken from Wechsler* et al. *(1976)*

†*Standard errors (1σ) are given in parentheses and refer to the estimated error in the least significant decimal places. This convention is followed in all tables.*

ter every 20 reflections, was found to diminish almost linearly with time. At the end of the heating period (~30 hours), the standard intensity had decreased to about 80 percent of its initial value. A check of the crystal orientation showed that misalignment was not the problem. Also, precession photographs taken at room temperature after heating revealed that only a single-phase armalcolite with sharp reflections was present. Thus, the decrease in intensity was not the result of decomposition. The decrease is believed to be due to platinum which evaporated from the heating device and was deposited on the sealed capillary enclosing the crystal. Metallic crystals were clearly visible on the outside of the capillary after the experiment. All the intensities for this data set were scaled up as a function of time to account for this effect.

Structure refinements were carried out using L. W. Finger's least-squares program RFINE2. Starting parameters were taken from Wechsler *et al.* (1976), atomic scattering factors for neutral atoms were used (Doyle and Turner, 1968), and reflections were weighted on the basis of counting statistics. The structures were initially refined varying one scale factor, positional parameters, and isotropic temperature factors. In subsequent cycles, anisotropic temperature factors were refined for all atoms and a secondary extinction parameter was refined. Both real and imaginary parts of the anomalous dispersion were included. The occupancy of a hypothetical composite $Fe_{0.5}Mg_{0.5}$ atom in the $M1$ site was allowed to vary in some models. Reflections with $F_{obs} < 3\sigma$ were rejected from the refinements. Final parameters for five refinements are reported in Table 2.

Structural details

Armalcolite has a pseudobrookite-type structure (Pauling, 1930; Hamelin, 1958), and its structural details have been described by Lind and Housley (1972), Smyth (1974), and Wechsler *et al.* (1976). Cations are accommodated in two symmetrically-distinct octahedrally-coordinated sites. The $M1$ site (Wyckoff notation 4c) is larger and more distorted than $M2$ (Wyckoff notation 8f), where polyhedral distortion is measured by the quadratic elongation (Robinson *et al.*, 1971). The two octahedral sites are linked by shared edges to form bands extending in the b direction. Previous studies have indicated that Ti predominates in the $M2$ site, while Fe and Mg are predominant in $M1$. However, Wechsler *et al.* (1976) suggested that significant disorder may exist in samples rapidly quenched from high temperature.

Selected bond distances and angles for all data sets are reported in Table 3, and mean M–O distances are summarized in Table 1. In Figure 1 the mean M–O distances for Arm-E refinements are compared, to depict the effects of annealing and thermal expansion on the size of the octahedral sites. The annealing at 400°C resulted in a large increase in the ⟨$M1$–O⟩ distance and a concomitant decrease in ⟨$M2$–O⟩. At 1100°C, the ⟨$M1$–O⟩ distance is actually smaller than at room temperature after annealing at 400°C. At room temperature after the 1100°C heating, the ⟨M–O⟩ distances are virtually the same as at room temperature before annealing. For Arm-C, ⟨$M2$–O⟩ is somewhat smaller at 400°C than at room temperature, while ⟨$M1$–O⟩ is substantially larger. These

Table 2. Final occupancy, positional, and thermal parameters for two synthetic armalcolites

		Arm-E				Arm-C
		24°C before annealing	24°C after annealing	1100°C	24°C after heating	400°C
M1	Fe	0.332(16)	0.456(16)	0.406(26)	0.367(36)	0.5
	Mg	0.332	0.456	0.406	0.367	0.5
	Ti	0.335	0.088	0.188	0.266	0
	x	0.80743(8)	0.80614(10)	0.81265(27)	0.80703(30)	0.80806(9)
	y	1/4	1/4	1/4	1/4	1/4
	z	0	0	0	0	0
	β_{11}	0.00139(8)	0.0017(1)	0.0060(3)	0.0024(3)	0.00279(8)
	β_{22}	0.00157(8)	0.0016(1)	0.0045(2)	0.0019(3)	0.00260(8)
	β_{33}	0.0194(7)	0.0116(8)	0.0401(24)	0.0172(24)	0.0310(7)
	$\beta_{12}=\beta_{13}=\beta_{23}$	0	0	0	0	0
	B_{eq}	0.75(2)	0.65(2)	2.16(7)	0.88(7)	1.29(2)
M2	Fe	0.084	0.022	0.047	0.066	0
	Mg	0.084	0.022	0.047	0.066	0
	Ti	0.832	0.956	0.906	0.867	1.0
	x	0.13464(5)	0.13370(6)	0.13470(17)	0.13428(19)	0.13394(5)
	y	0.43528(6)	0.43322(6)	0.43551(16)	0.43494(17)	0.43374(5)
	z	0	0	0	0	0
	β_{11}	0.00128(6)	0.00137(6)	0.00517(16)	0.00221(16)	0.00198(5)
	β_{22}	0.00174(6)	0.00140(6)	0.00560(17)	0.00160(15)	0.00263(5)
	β_{33}	0.0170(4)	0.0077(4)	0.0281(13)	0.0104(12)	0.0221(4)
	β_{12}	-0.00008(3)	-0.00004(4)	0.00002(13)	-0.00003(14)	-0.00003(3)
	$\beta_{13}=\beta_{23}$	0	0	0	0	0
	B_{eq}	0.71(1)	0.51(1)	1.98(4)	0.69(4)	1.02(1)
O1	x	0.2243(4)	0.2141(4)	0.2324(10)	0.2237(11)	0.2182(3)
	y	1/4	1/4	1/4	1/4	1/4
	z	0	0	0	0	0
	β_{11}	0.0038(3)	0.0026(3)	0.0078(10)	0.0023(10)	0.0044(3)
	β_{22}	0.0021(3)	0.0015(3)	0.0055(8)	0.0031(9)	0.0021(2)
	β_{33}	0.0242(22)	0.0120(24)	0.0578(88)	0.0073(68)	0.0288(21)
	$\beta_{12}=\beta_{13}=\beta_{23}$	0	0	0	0	0
	B_{eq}	1.22(7)	0.75(7)	2.86(24)	0.85(21)	1.37(6)
O2	x	0.0464(2)	0.0455(3)	0.0454(6)	0.0457(7)	0.0458(2)
	y	0.8846(2)	0.8866(3)	0.8841(6)	0.8842(7)	0.8862(2)
	z	0	0	0	0	0
	β_{11}	0.0020(2)	0.0017(2)	0.0062(7)	0.0032(7)	0.0018(2)
	β_{22}	0.0019(2)	0.0012(2)	0.0043(6)	0.0021(6)	0.0023(2)
	β_{33}	0.0311(17)	0.0202(18)	0.0888(75)	0.0150(51)	0.0506(19)
	β_{12}	-0.0002(2)	-0.00007(19)	0.00005(51)	0.00005(58)	0.0001(1)
	$\beta_{13}=\beta_{23}$	0	0	0	0	0
	B_{eq}	1.09(5)	0.75(5)	3.09(18)	0.97(15)	1.49(5)
O3	x	0.3133(2)	0.3141(3)	0.3121(7)	0.3132(7)	0.3146(2)
	y	0.9348(2)	0.9397(2)	0.9326(6)	0.9351(6)	0.9385(2)
	z	0	0	0	0	0
	β_{11}	0.0024(2)	0.0017(2)	0.0082(7)	0.0029(7)	0.0028(2)
	β_{22}	0.0030(2)	0.0024(2)	0.0079(7)	0.0028(6)	0.0042(2)
	β_{33}	0.0157(15)	0.0045(15)	0.0377(50)	0.0133(51)	0.0200(14)
	β_{12}	-0.0001(1)	0.00006(19)	-0.0003(7)	-0.0009(6)	0.0001(1)
	$\beta_{13}=\beta_{23}$	0	0	0	0	0
	B_{eq}	1.00(5)	0.63(5)	2.88(17)	1.00(16)	1.30(4)
	Space Group	*Bbmm*	*Bbmm*	*Bbmm*	*Bbmm*	*Bbmm*
	N(obs)	426	396	300	348	429
	R	0.034	0.031	0.078	0.081	0.028
	R(wt.)	0.043	0.037	0.059	0.078	0.041

Table 3. Selected bond distances (A) and angles (°) of two synthetic armalcolites

	Arm-E				Arm-C
	24°C before annealing	24°C after annealing	1100°C	24°C after heating	400°C
M1 Site					
M1-O1*	2.044(1)	2.075(2)	2.043(4)	2.043(4)	2.067(1)
M1-O2	1.966(2)	1.995(3)	1.960(7)	1.971(7)	1.980(2)
M1-O3	2.198(2)	2.240(3)	2.232(6)	2.199(7)	2.245(2)
<M1-O>	2.069	2.103	2.078	2.071	2.098
Quad. Elongation	1.0874	1.1048	1.0818	1.0881	1.0996
O1-O2	3.220(3)	3.298(3)	3.202(8)	3.225(9)	3.271(3)
O1-O3	2.662(2)	2.687(2)	2.682(5)	2.664(5)	2.685(2)
O2-O2	2.702(3)	2.749(4)	2.732(8)	2.694(10)	2.745(3)
O2-O3	2.657(3)	2.671(4)	2.686(9)	2.663(10)	2.677(3)
O3-O3	3.708(3)	3.818(4)	3.718(8)	3.717(9)	3.798(3)
O1-M1-O2	106.80(7)	108.26(7)	106.20(19)	106.91(20)	107.83(6)
O1-M1-O3	77.67(5)	76.93(6)	77.57(16)	77.71(16)	76.91(5)
O2-M1-O2	86.78(9)	87.1(1)	88.37(27)	86.23(31)	87.75(9)
O2-M1-O3	79.09(9)	77.99(9)	79.41(24)	79.17(27)	78.36(8)
O3-M1-O3	115.03(9)	116.9(1)	112.81(27)	115.43(29)	115.54(9)
M2 Site					
M2-O1'	2.055(2)	2.003(2)	2.122(5)	2.052(5)	2.026(1)
M2-O2	2.002(2)	2.006(3)	2.038(6)	2.012(7)	2.008(2)
M2-O2'	1.841(2)	1.809(3)	1.858(7)	1.831(8)	1.819(2)
M2-O3	2.180(2)	2.174(3)	2.211(7)	2.181(7)	2.184(2)
M2-O3'	1.9430(5)	1.9401(6)	1.955(2)	1.943(2)	1.9384(5)
<M2-O>	1.994	1.979	2.023	1.994	1.986
Quad. Elongation	1.0388	1.0400	1.0415	1.0393	1.0391
O1'-O2'	2.971(4)	2.879(4)	3.070(11)	2.957(12)	2.920(3)
O1'-O3	3.281(3)	3.271(3)	3.238(6)	3.280(7)	3.277(3)
O1'-O3'	2.662(2)	2.687(2)	2.682(4)	2.664(5)	2.685(2)
O2 -O2'	2.487(3)	2.449(4)	2.525(8)	2.492(10)	2.461(3)
O2 -O3'	2.946(3)	2.903(3)	3.003(7)	2.950(7)	2.913(2)
O2'-O3'	2.994(2)	2.979(3)	3.019(7)	2.989(8)	2.979(2)
O3 -O3'	2.600(2)	2.556(2)	2.635(6)	2.595(7)	2.575(2)
O1'-M2-O2'	99.22(12)	97.98(13)	100.75(31)	99.03(35)	98.69(11)
O1'-M2-O3	101.50(11)	103.01(13)	100.32(30)	101.54(33)	102.18(11)
O1'-M2-O3'	83.45(8)	85.90(8)	82.16(19)	83.59(21)	85.25(7)
O2 -M2-O2'	80.50(10)	79.68(11)	80.65(26)	80.70(30)	79.87(9)
O2 -M2-O3	78.78(9)	79.33(10)	78.29(25)	78.73(28)	79.27(9)
O2 -M2-O3'	96.62(7)	94.69(8)	97.51(19)	96.48(21)	95.11(7)
O2'-M2-O3'	104.54(7)	105.18(7)	104.72(20)	104.72(21)	104.88(6)
O3 -M2-O3'	77.98(7)	76.60(8)	78.19(20)	77.74(21)	77.05(7)
Cation-Cation					
M1-M2	3.2083(6)	3.2410(6)	3.245(2)	3.215(2)	3.2367(5)
M1-M2'	3.1347(6)	3.1184(7)	3.196(2)	3.132(2)	3.1338(6)
M2-M2	2.9355(7)	2.9321(9)	2.973(2)	2.931(3)	2.9372(7)
M2-M2'	3.2079(6)	3.2319(7)	3.237(2)	3.214(2)	3.2285(5)
Octah. Chain Edges					
O3-O3 -O1'	164.62(10)	162.66(11)	166.28(30)	164.55(31)	163.31(9)
O3-O1'-O3	149.23(13)	145.32(14)	152.55(37)	149.10(39)	146.61(12)

**Atom designations are those given in Wechsler* et al. *(1976). Symmetrically equivalent atoms are distinguished (e.g. O2 vs. O2') only for the purpose of identifying non-equivalent bond distances and angles.*

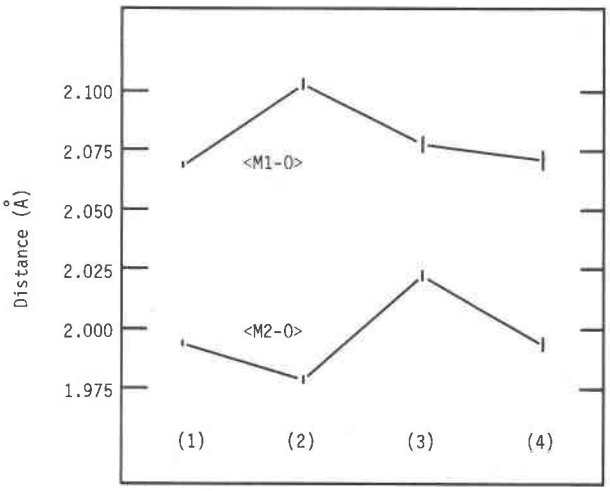

Fig. 1. Mean $M1$–O and $M2$–O distances of Arm-E. (1) Room temperature before annealing. (2) Room temperature after annealing at ~400°C for 24 hours. (3) 1100°C. (4) Room temperature after 1100°C heating. Length of symbols indicates estimated error ($\pm 1\hat{\sigma}$) in mean M–O distances.

observations may be indicative of the order-disorder present in the crystals as well as the thermal expansion at high temperatures.

The unit-cell parameters of Arm-E changed significantly as a result of the 24-hour annealing at 400°C (Table 1). The b dimension increased considerably, while a, c, and the unit-cell volume decreased. At room temperature after the 1100°C heating cycle, all values were intermediate between those of the first two sets of room-temperature values. For Arm-C, the data at 400°C indicate that the a and c cell dimensions were smaller than at room temperature, whereas b and the cell volume were increased. These trends appear to reflect the degree of cation ordering in the crystals, and indicate an apparent dependence of the b dimension on the size of the $M1$ site, while the a and c dimensions are dependent upon $M2$. An explanation for this behavior was previously suggested by Wechsler *et al.* (1976) on the basis of octahedral edge-sharing in the structure.

Cation distribution

In a previous paper (Wechsler *et al.*, 1976), the existence of significant cation disorder in synthetic armalcolite quenched from 1200°C was inferred from a consideration of expected and observed mean bond distances for the two cation sites. The data presented here provide further evidence supporting this argument.

Because of the size differences between Fe, Mg, and Ti, the mean M–O distances for the two cation sites are sensitive to the cation distribution. The mean M–O distances predicted on the basis of Shannon and Prewitt's (1969) radii for Fe^{2+}, Mg^{2+}, and Ti^{4+} (octahedrally coordinated) for two hypothetical cation distributions are presented in Table 4. The $\langle M\text{–O}\rangle$ distances observed for Arm-E at room temperature before annealing closely resemble those predicted for the disordered cation distribution shown in Table 4. After annealing at ~400°C for 24 hours, the second room-temperature data set indicates an increase in $\langle M1\text{–O}\rangle$ and decrease in $\langle M2\text{–O}\rangle$, resulting in bond distances closer to those predicted for the completely-ordered distribution. Thus the first room-temperature data set indicates that significant cation disorder was retained after the initial quench from 1200°C when the crystal was synthesized. Annealing at 400°C resulted in migration of the larger cations, Fe and Mg, into $M1$ and the smaller Ti into $M2$. The subsequent decrease in $\langle M1\text{–O}\rangle$ noted in the refinement at 1100°C is interpreted as resulting from the reappearance of cation disorder at high temperature. After quenching to room temperature, the $\langle M\text{–O}\rangle$ distances resemble those for the first room-temperature data set, indicating that the disorder was again quenched in.

The data for Arm-C collected at 400°C indicate similar trends. The size of the $\langle M1\text{–O}\rangle$ increase over room temperature is difficult to explain as simple

Table 4. Predicted $\langle M\text{–O}\rangle$ distances for two possible cation distributions

Ionic radii (Å), from Shannon and Prewitt (1969):

$^{VI}Fe^{2+}$	0.77	$^{III}O^{2-}$	1.36
$^{VI}Mg^{2+}$	0.72	$^{IV}O^{2-}$	1.38
$^{VI}Ti^{4+}$	0.605		

		ordered	partially disordered
M1	Fe	0.5	0.333
	Mg	0.5	0.333
	Ti	---	0.333
	<M1-O>	2.118	2.072
M2	Fe	---	0.083
	Mg	---	0.083
	Ti	1.0	0.833
	<M2-O>	1.978	2.001

thermal expansion, and the $\langle M2\text{–O}\rangle$ decrease is unlikely to be a thermal effect. Rather, the $\langle M\text{–O}\rangle$ distances are consistent with strong ordering of Fe and Mg into $M1$ and Ti into $M2$ at this temperature. It should be noted that intracrystalline cation diffusion apparently takes place at this relatively low temperature under conditions where armalcolite is expected to be a metastable phase (Lindsley *et al.*, 1974). Apparently the kinetics of the decomposition reaction are unfavorable, at least over a period of ~24 hours, at this temperature. However, the precession-camera studies indicate that decomposition does occur at 600°C.

In an attempt to further quantify the degree of cation disorder in each of the data sets, the cation occupancy of the $M1$ site was refined. Since the occupancies of three cations in two sites are not readily determined by the least-squares techniques used, a simplifying assumption had to be made. Rather than fix either Fe, Mg, or Ti in either of the cation sites, it was decided to allow Fe and Mg to vary together. This was accomplished by including a scattering curve for a hypothetical $Fe_{0.5}Mg_{0.5}$ atom in the refinement procedure and allowing the occupancy of this atom in the $M1$ site to vary. The total occupancy of both sites and the total amounts of Fe, Mg, and Ti were kept fixed. Although this may not model the true exchange behavior precisely, it is expected to provide a useful indication of the probable degree of disorder. It should also be noted that the Fe–Mg composite atom is similar in X-ray scattering power to pure Ti, and the refinements are therefore not particularly sensitive to these occupancy parameters.

For each data set, the refinement was first carried out with a completely ordered distribution model, with all Fe and Mg in $M1$ and all Ti in $M2$. This was followed by a refinement in which the Fe–Mg occupancy of $M1$ was allowed to vary. For Arm-E partially-disordered distributions were obtained for all data sets, and the refined occupancy values are given in Table 2. For Arm-C at 400°C, the occupancy of Fe–Mg in $M1$ became slightly greater than 1.0 in the refinement, although statistical parameters indicated no significant difference between the ordered and disordered models. Therefore the ordered model with fixed occupancies is presented in Table 2.

The statistical parameters for the refinement of room-temperature data before annealing indicate the disordered model is a significant improvement over the completely-ordered model (Table 5). The occupancies thus determined agree well with the prediction made on the basis of bond distances. In the other three data sets for Arm-E no significant difference in the fit was found for the ordered and disordered models. For the room-temperature data set after annealing, where the R-factors and errors are comparable to those of the first room-temperature data set, this is consistent with a completely or nearly completely ordered cation distribution. For the data at 1100°C and at room temperature after heating, the refinements are not sufficiently precise to determine the cation occupancies reliably, given the similarity in scattering power between Ti and Fe + Mg. If the occupancies determined for these cases were taken at face value, they would indicate greater disorder at room temperature after heating than at 1100°C, which is highly unlikely. Rather, the errors in these two data sets are too large to define the cation distribution accurately by this technique. However, the results are certainly consistent with the inferences about cation disorder made from the bond distances. Since positional parameters are in general more precisely determined by least-squares refinements than are occupancies, the bond distances are expected to be better determined than the refined occupancies.

Table 5. Comparison of residuals for two occupancy models of Arm-E at 24°C before annealing

	(1)	(2)
N_{obs}	426	426
R	0.035	0.034
R(wt.)	0.048	0.043
Standard Deviation of Unit Weight Obs.	2.33	2.12

(1) Fixed occupancies, ordered distribution model

(2) Occupancy refined

Although the cation distribution at 1100°C cannot be determined directly by X-ray methods, the mean M–O distances at that temperature may indicate the relative degree of disordering. The greater similarity between $\langle M1\text{–O}\rangle$ and $\langle M2\text{–O}\rangle$ at 1100°C than at room temperature (based on mean atomic positions, uncorrected for thermal motion) suggests the possibility that the cation distribution is indeed somewhat more disordered at 1100°C than after 'quenching' to room temperature, as might be expected. However, the effects due to thermal expansion of Fe–O, Mg–O, and Ti–O would need to be evaluated independently before this interpretation could be verified.

Discussion

These results argue in favor of the existence of substantial cation disorder in synthetic armalcolite at 1100–1200°C. Although the cation distributions cannot be uniquely defined by either M–O distance data or occupancy refinement techniques, the trends noted for annealing experiments and high-temperature structure refinements are best explained by a disordered cation distribution above 1100°C and relatively rapid diffusion and a nearly completely ordered cation distribution at 400°C. Considering that in a completely disordered cation distribution both cation sites would be occupied by ⅓[Fe + Mg] and ⅔Ti, the 'disordered' distributions found for quenched samples ($M1$ = ⅔[Fe + Mg] and ⅓Ti) actually represent half-disordered models, *i.e.* the disorder is halfway to completion.

Virgo and Huggins (1975) presented Mössbauer spectral data for armalcolite synthesized at 1100°C indicating ~42.3 percent of Fe^{2+} in the $M2$ site. This finding, although indicating a somewhat greater degree of disorder, is consistent with the semi-quantitative estimates made in this study. It is difficult to make a direct comparison between these results, since the samples were synthesized separately and may have experienced different cooling histories. Nevertheless, the observed M–O distances for Arm-E and Arm-C can be easily reconciled to the Fe^{2+} distribution measured by Virgo and Huggins on their samples.

The observations of cation disorder reported here are in agreement with the suggestion of Navrotsky (1975) that configurational entropy is an important factor in determining the stability relations of pseudobrookite-type and related minerals. With declining temperature, the equilibrium cation distribution would be expected to become more ordered, leading to a decrease in this stabilizing effect. Additional experiments are required to evaluate the effects of Cr^{3+}, Al^{3+}, and Ti^{3+} on the cation distribution at high temperatures and to determine the nature of their stabilizing influence on armalcolite.

Smyth (1974) and Wechsler *et al.* (1976) reported structure refinements of natural lunar armalcolites. Mean M–O distances found for the lunar armalcolites are quite similar to those determined for Arm-E after annealing at ~400°C for 24 hours, and are indicative of virtually complete cation ordering. The data presented here suggest that the highly ordered distributions found in lunar armalcolites may be the result of equilibration at relatively low temperatures. Further study of the kinetics of intracrystalline diffusion and thermal decomposition, as well as the effect of temperature on the equilibrium cation distribution, is needed to characterize more fully the subsolidus behavior of armalcolite and to evaluate its usefulness as an indicator of cooling history.

Acknowledgments

I thank J. J. Papike and C. T. Prewitt for their encouragement and guidance as well as for helpful discussions and reviews of the manuscript. A review by Joseph R. Smyth improved the manuscript. The cheerful assistance of Kay Tousley is also gratefully acknowledged. This work was supported by NASA Grant NGL 33-015-130.

References

Doyle, P. A. and P. S. Turner (1968) Relativistic Hartree-Fock X-ray and electron scattering factors. *Acta Crystallogr., A24,* 390–397.

El Goresy, A., P. Ramdohr, O. Medenbach and H.-J. Bernhardt (1974) Taurus-Littrow TiO_2-rich basalts: opaque mineralogy and geochemistry. *Proc. 5th Lunar Sci. Conf., Geochim. Cosmochim. Acta, Suppl. 5,* 627–652.

Haggerty, S. E. (1973) Armalcolite and genetically associated opaque minerals in the lunar samples. *Proc. 4th Lunar Sci. Conf., Geochim. Cosmochim. Acta, Suppl. 4,* 777–797.

Hamelin, M. (1958) The structure of the composition TiO_2-Al_2O_3, in comparison with pseudobrookite. *Bull. Soc. Chim. France, 1958,* 1559–1566.

Kesson, S. E. and D. H. Lindsley (1975) The effects of Al^{3+}, Cr^{3+}, and Ti^{3+} on the stability of armalcolite. *Proc. 6th Lunar Sci. Conf., Geochim. Cosmochim. Acta, Suppl. 6,* 911–920.

Lind, M. D. and R. M. Housley (1972) Crystallization studies of lunar igneous rocks: crystal structure of synthetic armalcolite. *Science, 175,* 521–523.

Lindsley, D. H., S. E. Kesson, M. J. Hartzman and M. K. Cushman (1974) The stability of armalcolite: experimental studies in the system MgO–Fe–Ti–O. *Proc. 5th Lunar Sci. Conf., Geochim. Cosmochim. Acta, Suppl. 5,* 521–534.

Navrotsky, A. (1975) Thermodynamics of formation of some compounds with the pseudobrookite structure and of the $FeTi_2O_5$–Ti_3O_5 solid solution series. *Am. Mineral., 60,* 249–256.

Papike, J. J., A. E. Bence and D. H. Lindsley (1974) Mare basalts from the Taurus-Littrow region of the moon. *Proc. 5th Lunar Sci. Conf., Geochim. Cosmochim. Acta, Suppl. 5,* 471–504.

Pauling, L. (1930) The crystal structure of pseudobrookite. *Z. Kristallogr., 73,* 97–112.

Robinson, K., G. V. Gibbs and P. H. Ribbe (1971) Quadratic elongation: a quantitative measure of distortion in coordination polyhedra. *Science, 172,* 567–570.

Shannon, R. D. and C. T. Prewitt (1969) Effective ionic radii in oxides and fluorides. *Acta Crystallogr., B25,* 925–946.

Smyth, J. R. (1974) The crystal chemistry of armalcolites from Apollo 17. *Earth Planet. Sci. Lett., 24,* 262–270.

Virgo, D. and F. E. Huggins (1975) Cation distributions in some compounds with the pseudobrookite structure. *Carnegie Inst. Wash. Year Book, 74,* 585–590.

Wechsler, B. A., C. T. Prewitt and J. J. Papike (1976) Chemistry and structure of lunar and synthetic armalcolite. *Earth Planet. Sci. Lett., 29,* 91–103.

Manuscript received, December 15, 1976; accepted for publication, May 12, 1977.